Increased Levels of a Unique Post-Translationally Modified βIVb-Tubulin Isotype in Liver Cancer†

Leah M. Miller,‡ Anuradha Menthena,‡ Champak Chatterjee,§ Pascal Verdier-Pinard,⊥ Phyllis M. Novikoff,|| Susan Band Horwitz,⊥ and Ruth Hogue Angeletti*,‡

Departments of Developmental and Molecular Biology, Pathology, and Molecular Pharmacology, Albert Einstein College of Medicine, Bronx, New York 10461, and Laboratory of Synthetic Protein Chemistry, The Rockefeller University, New York, New York 10065

Received March 26, 2008; Revised Manuscript Received May 23, 2008

ABSTRACT: Identifying changes at the molecular level during the development of hepatocellular carcinoma is important for the detection and treatment of the disease. The characteristic structural reorganization of preneoplastic cells may involve changes in the microtubule cytoskeleton. Microtubules are dynamic protein polymers that play an essential role in cell division, maintenance of cell shape, vesicle transport, and motility. They are comprised of multiple isotypes of α- and β-tubulin. Changes in the levels of these isotypes may affect not only microtubule stability and sensitivity to drugs but also interactions with endogenous proteins. We employed a rat liver cancer model that progresses through stages similar to those of human liver cancer, including metastasis to the lung, to identify changes in the tubulin cytoskeleton during carcinogenesis. Tubulin isotypes in both liver and lung tissue were purified and subsequently separated by isoelectric focusing electrophoresis. The C-terminal isotype-defining region from each tubulin was obtained by cyanogen bromide cleavage and identified by mass spectrometry. A novel post-translational modification of βIVb-tubulin in which two hydrophobic residues are proteolyzed from the C-terminus, thus exposing a charged glutamic acid residue, was identified. The unique form of βIVb-tubulin was quantified in the liver tissue of all carcinoma stages and found to be approximately 3-fold more abundant in nodular and tumor tissue than in control tissue. The level of this form was also found to be increased in lung tissue with liver metastasis. This modification alters the C-terminal domain of one of the most abundant β-tubulin isotypes in the liver and therefore may affect the interactions of microtubules with endogenous proteins.

Microtubules are dynamic protein polymers that play an essential role in cell division, maintenance of cell shape, transport of vesicles, and cell motility (*1*). These hollow cylinders are constructed of heterodimers of α- and β-tubulin, which bind in a head-to-tail fashion to form protofilaments that associate laterally to form microtubules (*2*). There are six α-tubulin and seven β-tubulin genes described in mammals, with each gene being highly conserved across species (*3*). The majority of the diversity in tubulin gene products, termed isotypes, occurs in the last 15−20 residues of the C-terminus, which is known as the isotype-defining region and is located on the outer surface of microtubules (*4*). Further increasing the diversity of the tubulin isotypes is their ability to undergo a range of post-translational modifications. Common post-translational modifications of tubulin are polyglutamylation, tyrosination/detyrosination, polyglycylation, acetylation, and phosphorylation, most of which occur in the C-terminal region (*5*). Although there is no consensus regarding the specific role or function of individual tubulin isotypes, tissue-specific changes in the expression of tubulin isotypes have been observed, and isotype composition has been demonstrated to affect the dynamics of microtubule assembly (*6–8*). It has been suggested that divergent C-termini may provide a mechanism for isotype-specific microtubule-associated protein (MAP) binding (*9*). Recently, a tubulin code, similar to the histone code, was proposed in which tubulin isotypes and their modifications could serve as discrete signals in modulating cellular events, suggesting a mechanistic role for the observed diversity in microtubules (*10*).

The integrity of the cytoskeleton is essential for the proper functioning of all cells. Therefore, changes in the composition of microtubules, a major component of the cytoskeleton, could contribute to tumorigenesis. Previous studies have examined the α- and β-tubulin isotypes in both tumors and cancer cell lines. An increase in the level of βIII-tubulin is the most commonly described alteration in tubulin expression in cancer, with an increase of this neuronal isotype observed in a variety of tumors (*11–15*). An increase in the level of expression of the βII-tubulin in cancer has also been

† Supported by NIH Grants CA06576 (to P.M.N.), CA077263 and CA124898 (to S.B.H.), and CA101150 (to R.H.A.). L.M.M. was supported by an NRSA training grant (DK07218) and a postdoctoral fellowship (CA125923).

* To whom correspondence should be addressed. E-mail: angelett@aecom.yu.edu. Telephone: (718) 430-3475. Fax: (718) 430-8939.

‡ Department of Developmental and Molecular Biology, Albert Einstein College of Medicine.

§ The Rockefeller University.

|| Department of Pathology, Albert Einstein College of Medicine.

⊥ Department of Molecular Pharmacology, Albert Einstein College of Medicine.

10.1021/bi8005225 CCC: $40.75
Published on Web 06/21/2008

described previously (*16*). While a majority of studies have focused on β-tubulins, a recent report demonstrated a shift in post-translational modifications of α-tubulin isotypes in prostate cancer cell lines (*17*). In these studies, isotypes were assigned either at the protein level using isotype-specific antibodies or at the mRNA level by RT-PCR. Both of these methods continue to provide important qualitative and quantitative data about tubulin isotypes. However, neither method is able to completely describe the tubulin isotypes at the protein level.

Mass spectrometry (MS)[1] complements traditional methods of characterizing tubulin isotypes (*18*). It is an ideal tool for the identification of post-translational modifications of tubulins, with the ability to characterize multiple modifications in one experiment (*19, 20*). Unlike experiments employing antibodies, mass spectrometry can be used to detect mutations in isotypes as well as to identify new isotypes (*21, 22*). Also, when combined with "stable isotope labeling with amino acids in culture" (SILAC), mass spectrometry provides information regarding the relative expression levels of tubulin isotypes in drug resistant cell lines as compared to the tubulin isotypes present in drug sensitive cell lines (*23*). Therefore, the application of mass spectrometry to tubulin isotype characterization can provide unique information about tubulin isotypes at the protein level that cannot readily be achieved with other methods.

Using a highly reproducible rat liver cancer model, the resistant hepatocyte model, we profiled the tubulin isotypes present at early, middle, and late stages of cancer development (*24*). Hepatocellular carcinoma (HCC) is one of the most common and fatal forms of cancer worldwide (*25*). Detection of HCC at early stages is difficult, and treatment options after identification are limited and often ineffective (*26*). To gain a better understanding of the changes occurring at the molecular level in carcinogenesis, we employed high-resolution isoelectric focusing along with cyanogen bromide (CNBr) cleavage and MS to identify the tubulin isotypes present in the liver. Our methodology allowed for the identification of a novel C-terminal modification to βIVb-tubulin. We quantitated the relative amount of the peptide harboring this novel post-translational modification compared to all β-tubulin isotypes, and when comparing the levels in rat liver which underwent chemical carcinogen treatment relative to control liver, we demonstrated a 3-fold increase in the level of modification during later stages of cancer. Such changes in a post-translational modification of a tubulin isotype during progression of liver cancer suggest that alterations to microtubules may be a useful indicator for the detection and treatment of liver cancer.

MATERIALS AND METHODS

Materials. Male Fisher F344 rats, 120−130 g in weight on arrival, were purchased from Charles River Laboratories (Wilmington, MA). All animal studies were conducted under protocols approved by the Animal Care and Use Committee of the Albert Einstein College of Medicine in accordance with National Institutes of Health guidelines. For all surgical procedures, animals were anesthetized using isoflurane gas and for sacrifice a lethal dose of CO_2 was administered (10−15 psi). Chemical carcinogens were from Sigma-Aldrich and Innovative Research of America (Sarasota, FL). Paclitaxel (Taxol) was obtained from the Drug Development Branch of the National Cancer Institute (Bethesda, MD), dissolved in sterile dimethyl sulfoxide, and stored at −20 °C. All other chemicals were obtained from Sigma (St. Louis, MO), except where otherwise noted.

Generation of a Resistant Hepatocyte Rat Model. The Solt-Farber chemical carcinogen protocol was used for inducing sequential stages of hepatic cancer in rats (*24, 27*). Briefly, the protocol consisted of administering two different carcinogens, diethylnitrosamine (DEN) and 2-acetylaminofluorene (AAF), and a surgical two-thirds partial hepatectomy. Animals were allowed to acclimatize for 1 week at the animal facility before the protocol was initiated. A single intraperitoneal injection of DEN at a dose of 200 mg/kg of body weight was injected into the rats, and 2 weeks later, AAF in the form of a single pellet designed to release a total of 35 mg of AAF over a 14 day period was surgically inserted subcutaneously in the back of the neck. One week after insertion of the pellet, partial hepatectomy was performed under anesthesia. Following this regenerative stimulus, a sequential development of nodules and hepatomas occurred. To obtain early and late stages of liver cancer and metastasis to lung, animals were sacrificed 9 days, 4 months, 6 months, and 10 months after partial hepatectomy. These stages corresponded to those described by Solt-Farber, namely, preneoplastic nodules, early and late persistent nodules, and hepatoma, respectively. Each stage could be easily identified on gross examination of the liver. Control animals that either underwent a partial hepatectomy (9 day control) or received a surgical incision to induce surgical stress (sham operated) were sacrificed at each stage. All animals were fasted overnight prior to being sacrificed. Liver and lung were removed from animals within 10 min after they were sacrificed. For tubulin analyses, pieces of the liver from the right lateral lobe were snap-frozen in liquid nitrogen and crushed with a mortar and pestle. For cryostat sections, pieces of liver from the same lobe and lung were snap-frozen in methylbutane. For tubulin analysis of lung, hand-sliced sections of the lung were made from the methylbutane frozen tissue.

Purification of Tubulin from Liver Tissue. Paclitaxel-stabilized microtubule pellets were prepared using a modified version of a previously described method (*21*). One and one-half volumes of MES glutamate buffer [0.1 M 2-(*N*-morpholino)ethanesulfonic acid (pH 6.8), 0.5 mM $MgCl_2$, 1 mM EGTA, and 1 M glutamate] was used to resuspend the powdered tissue. A protease inhibitor cocktail (Roche, Indianapolis, IN) (one tablet dissolved in 1 mL of MES glutamate buffer) was added at $^1/_{10}$ the total volume, and DTT was added to a final concentration of 1 mM before the tissue was disrupted via sonication. The cellular debris was pelleted at 30000*g* (Beckman TLA 100.3 rotor) at 4 °C for 15 min and then the supernatant centrifuged at 120000*g* at 4 °C for 1 h. Paclitaxel was added to the cleared supernatant

[1] Abbreviations: MS, mass spectrometry; HCC, hepatocellular carcinoma; CNBr, cyanogen bromide; IPG, immobilized pH gradient; SDS−PAGE, sodium dodecyl sulfate−polyacrylamide gel electrophoresis; DEN, diethylnitrosamine; AAF, 2-acetylaminofluorene; DTT, dithiothreitol; FA, formic acid; IEF, isoelectric focusing; pI, isoelectric point; MALDI-TOF/TOF, matrix-assisted laser desorption ionization tandem time-of-flight; EST, expressed sequence tag; MS/MS, tandem mass spectrometry; ESI-MS, electrospray ionization mass spectrometry; SNPs, single-nucleotide polymorphisms.

to a final concentration of 20 μM along with 1 mM GTP and incubated at 37 °C for 30 min. This solution was layered onto a 100 μL cushion containing 20% sucrose in MES glutamate buffer and 20 μM paclitaxel and centrifuged at 30000*g* for 30 min at 37 °C. The pellet containing the microtubules was resuspended in 30 μL of MES glutamate buffer containing 0.35 M NaCl and 20 μM paclitaxel and was incubated at 37 °C for 10 min. The microtubules were pelleted by centrifugation at 30000*g* for 30 min at 37 °C, and the supernatant was removed and the pellet flash-frozen on liquid nitrogen and stored at −80 °C.

Isoelectric Focusing. Paclitaxel-stabilized microtubule pellets (~15 μg) were dissolved in 500 μL of solubilization buffer {7 M urea, 2 M thiourea, 4% 3-[3-(cholamidopropyl)dimethylammonio]-1-propanesulfonate, 0.5% Triton X-100, 0.5% ampholyte-containing buffer (pH 4.5−5.5), 20 mM DTT, and bromophenol blue}. The sample was loaded onto 24 cm IPG strips (pH 4.5−5.5, GE Healthcare Life Sciences, Piscataway, NJ) and run on an IPGphor II IEF system for a total of 65000 Vh. The IPG strips were fixed and stained using the Colloidal Blue Staining Kit (Invitrogen, Carlsbad, CA). Following staining, strips were scanned and bands corresponding to tubulin were cut from the gels.

CNBr Cleavage of Tubulin and MS Analysis. Each IEF gel piece was destained and then vacuum-dried. The dried bands were rehydrated in 100 μL of CNBr (70% formic acid and 100 mg/mL CNBr), cleaved overnight at room temperature in the dark, and then the solvent vacuum-dried. The peptides were washed with 100 μL of 50% acetonitrile containing 0.3% TFA, vacuum-dried, washed with 50 μL of the same solution, and dried. Before MS analysis, the peptides were dissolved in 10 μL of 50% acetonitrile containing 0.3% TFA, and 0.5 μL was mixed with 0.5 μL of saturated sinapic acid (in 50% acetonitrile and 0.1% TFA) and deposited onto a MALDI target. MS analysis was performed in negative ion mode on an ABI 4700 MALDI-TOF/TOF mass spectrometer (Applied Biosystems, Foster City, CA) as described previously (*23*). MS/MS analysis was performed in positive ion mode on the same instrument. MS/MS data were searched against protein (NCBI and MSDB) and EST databases using the Mascot search engine.

Synthesis of ^{15}N-Labeled Internal Standards. Commercially available ^{15}N-labeled Gly, Leu, and Ala (Cambridge Isotopes, Andover, MA) were protected with the base-labile Fmoc (fluorenylmethoxycarbonyl) group following reported procedures (*28*). Two peptides bearing these labeled amino acids were synthesized on the solid phase employing a standard Fmoc-based protection strategy. The first peptide was an internal β-tubulin peptide common to the βI, βII, βIVb, and βV isotypes (**G**T**LL**ISKIREEYPDRIMNT, bold residues include the ^{15}N label). The second peptide had the same sequence as the novel C-terminal β-tubulin peptide obtained by CNBr cleavage (ND**L**VSEYQQYQD**A**T**A**EEE**G**EFEEE-**A**EEE). Following chain assembly, peptide cleavage from the resin was undertaken with a cocktail consisting of trifluoroacetic acid, triisopropylsilane, water, and anisole (92.5:2.5:2.5:2.5) and the crude peptides purified by C18 semipreparative reversed phase HPLC employing a gradient of 25 to 50% B (A, H_2O and 0.1% TFA; B, 90% acetonitrile and 0.1% TFA in H_2O) over 45 min. Fractions containing the desired peptides were identified by ESI-MS and lyophilized prior to use. The internal peptide standard was synthesized with two additional C-terminal residues following the methionine such that CNBr fragmentation would lead to formation of the homoserine lactone identical to that observed in assay samples (*29*).

Quantitation of the Novel β-Tubulin Post-Translational Modification. Tubulin pellets were resuspended in 20 μL of 25 mM Tris (pH 6.8) and 1% SDS, and the total protein concentration was determined by the BCA assay (Pierce, Rockford, IL). For each sample, 7.5 μg of protein was loaded onto a 12% SDS−PAGE gel (Bio-Rad, Hercules, CA) and run at a constant voltage (150 V). The gels were stained with GelCode Blue Stain Reagent (Pierce, Rockford, IL) and scanned. The band containing all tubulin isotypes (as indicated by the 50 kDa molecular mass marker) was cut from the gel, destained, and vacuum-dried. Before CNBr cleavage, 3 μL of a stock solution of the ^{15}N-labeled peptide standards (5 μM internal peptide and 2 μM C-terminal peptide) was added to each tube, and then 80 μL of CNBr solution (70% formic acid and 100 mg/mL CNBr) was added to each tube and the sample cleaved for 22−24 h at room temperature in the dark. The solution was removed and kept on ice, and the peptides were extracted from the gel twice via incubation at 37 °C with 100 μL of 70% acetonitrile and 0.1% TFA for 30 min. After each extraction, the supernatant was removed and added to the original supernatant. Following extraction, the sample was vacuum-dried, resuspended in 100 μL of 50% acetonitrile and 0.3% TFA, dried, resuspended in 50 μL of 50% acetonitrile and 0.3% TFA, and dried. The peptides were resuspended in 10 μL of H_2O with 0.1% TFA, purified on a C18 ZipTip (Millipore, Billerica, MA), and eluted into 4 μL of 70% acetonitrile and 0.1% TFA. The sample (0.5 μL) was mixed with 0.5 μL of saturated sinapic acid and spotted onto a MALDI target.

The CNBr-generated peptide mixture containing the internal standards was analyzed in both positive (internal peptide) and negative ion mode (C-terminal peptide) via MALDI-TOF/TOF MS. After the data had been collected, each spectrum was processed in Data Explorer using the Advanced Baseline Correction and Noise Filtering functions. The region of each spectrum containing the peptide of interest was saved as an ASCII file and then plotted in Excel. The intensity for the highest isotope for each internal standard was set to 100. The isotope intensity values were then corrected to account for the overlap of the naturally occurring isotopic cluster with the standard isotopic cluster. The theoretical distribution of each peptide was calculated using the Exact Mass Calculator (FTMS Systems, Varian Inc., Lake Forest, CA), and the peak heights of the isotopes of the naturally occurring peptides were determined relative to the most abundant isotope. The isotopic abundance of the naturally occurring peptide was then subtracted from the full isotope pattern of the standard to obtain the corrected peak heights. Then, the total intensity for the unlabeled peptide (naturally occurring peptide) and the labeled peptide (internal standard) was determined by adding the intensity for the top three (internal peptide) or five (C-terminal peptide) isotopes of each isotopic cluster. The ratio of unlabeled to labeled was then calculated by dividing the total intensity of the unlabeled peptide by the total intensity of the labeled peptide. This was done for both the internal peptide and the C-terminal peptide. The ratio of β*-tubulin to total β-tubulin was obtained by dividing the value for the C-terminal peptide

Table 1: Isoelectric Points and C-Terminal Sequences for Tubulin Isotypes from *Rattus norvegicus*

tubulin isotype	gene	accession number	pI[a]	mass (Da)	mass (Da) of the C-terminal peptide	CNBr C-terminal peptide
α1A[b]	Tuba1a	AAA42306	4.94	50135.6	2860.193[c]	AALEKDYEEVGVDSVEGEGEEEGEEY
α1B	Tuba1b	AAH60572	4.94	50151.6	2860.193[c]	AALEKDYEEVGVDSVEGEGEEEGEEY
α1C	Tuba1c	AAH78829	4.96	49937.3	2590.035	AALEKDYEEVGADSAEGDDEGEEY
α3A	Tuba3a	EDM01850	4.98	49959.5	4150.766	EEGEFSEAREDLAALEKDYEEVGVDSVEAEAEEGEEY
α4A	Tuba4a	AAH83726	4.95	49924.4	2633.066	AALEKDYEEVGIDSYEDEDEGEE
α8	Tuba8	AAH79185	4.98	50037.5	4156.719	EEGEFSEAREDLAALEKDYEEVGTDSFEEENEGEEF
βI	Tubb5	CAE84031	4.78	49670.8	3366.333	NDLVSEYQQYQDATAEEEEDFGEEAEEEA
βII[d]	Tubb2b	AAI05755	4.78	49907.0	3466.360	NDLVSEYQQYQDATADEQGEFEEEEGEDEA
		CAA27067	4.79	49963.1	3480.376	NELVSEYQQYQDATADEQGEFEEEEGEDEA
βIII	Tubb3	AAH97281	4.82	50418.6	1610.622	YEDDDEESEAQGPK
βIVa	Tubb4	EDL83577	4.78	49585.8	3350.375	NDLVSEYQQYQDATAEEGEFEEEAEEEVA
βIVb	Tubb2c	AAH60597	4.79	49801.0	3479.417	NDLVSEYQQYQDATAEEEGEFEEEAEEEVA
βV	Tubb6	AAH97977	4.80	50059.3	3765.508	NDLVSEYQQYQDATVNDGEEAFEDEDEEEINE
βVI	LOC679312	XP_001055765	5.00	50416.1	769.335	GAEDKNH

[a] The isoelectric point, protein molecular mass, and CNBr peptide mass were all calculated using the ExPaSy PeptideMass tool. The protein molecular mass is reported as an average mass, and the masses of the C-terminal peptides are monoisotopic. The sequence for each tubulin isotype was found in the NCBI database using the given accession numbers. [b] α-Tubulin nomenclature follows the recently revised nomenclature for the α-tubulin gene family (*50*). [c] The α1A and α1B tubulin isotypes have the same CNBr C-terminal peptide and therefore cannot be distinguished from one another on the basis of the C-terminal peptide mass. [d] Two entries with distinct C-terminal sequences were found in the database for βII.

by the value of the internal peptide. Three different animals were examined at each stage and the final ratios averaged. This ratio was then compared to a set of control samples (prepared in the same way; ratios determined as described above) to establish the amount of the novel form of β-tubulin in the nodule or tumor tissue as compared to control animals. Three control animals were used for each stage.

RESULTS

Isotype Assignment by High-Resolution Isoelectric Focusing and CNBr Cleavage. Previous studies have demonstrated the ability of narrow-range isoelectric focusing to resolve tubulin isotypes differing in pI by as little as 0.01 (*21, 23*). The β-tubulin isotypes of rat have predicted pIs within the range of 4.78−5.00, with the majority falling between 4.78 and 4.82, and the α-tubulin isotypes have predicted pIs in the range of 4.94−4.98 (Table 1). Post-translational modifications, such as glutamylation (+E, +129 Da) and tyrosination/detyrosination (±Y, ±163 Da), further expand the diversity of the C-terminal peptides and shift the isoelectric points of the isotypes (*5*). On the basis of predicted isoelectric points, the β-tubulin isotypes should cluster in the more acidic region of the gel, with the α-tubulin isotypes present at the more basic region of the gel. A method employing high-resolution isoelectric focusing was used to determine the tubulin isotypes present in liver tissue (Figure 1). Figure 2A shows an example of the tubulin pellet purified from a control rat liver and separated on a 24 cm pH 4.5−5.5 isoelectric focusing gel. After the samples had been stained with Coomassie blue, 15 bands were cut from the gel and cleaved with CNBr. CNBr releases the unique C-terminal peptides from both α- and β-tubulin (Table 1), and these peptides ionize efficiently in negative ion mode mass spectrometry due to their acidic nature, thus facilitating the identification of C-terminal specific peptides (*22*). Figure 2B displays the negative ion mode MALDI-TOF spectrum for band 12 after CNBr cleavage. The C-terminal peptides are labeled with the corresponding isotype assignment. In the gel in Figure 2A, three β-tubulin and four α-tubulin isotypes were identified, as well as post-translationally modified forms of predicted C-terminal peptides. In a few cases, the bands

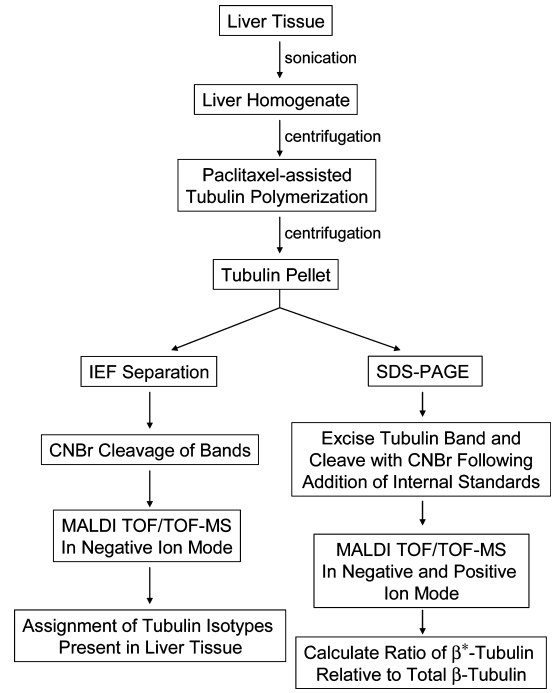

FIGURE 1: Strategies employed to identify tubulin isotypes and to quantitate the amount of the β* form of tubulin relative to total β-tubulin.

cut from the gel either did not contain tubulin or did not contain enough tubulin for identification. Some isotypes are observed in more than one band, which is most likely due to incomplete resolution of the IEF gel or post-translational modifications occurring outside the C-terminal tail, such as acetylation, or to sequence mutations (*5, 21*).

Identification of Novel Post-Translational Modification of a β-Tubulin C-Terminal Peptide. Isoelectric focusing experiments were able to resolve many different forms of tubulin. In all of the isoelectric focusing gels, a distinct band (Figure 3A, ↓β*) was observed at a pI slightly higher than that of βIVb, but this band could not be assigned to a known isotype or modified C-terminal peptide. After CNBr cleavage of this band, a peak corresponding to βIVb was observed in the negative ion mode mass spectrum as well as other peaks corresponding to β-tubulin internal peptides, but these did

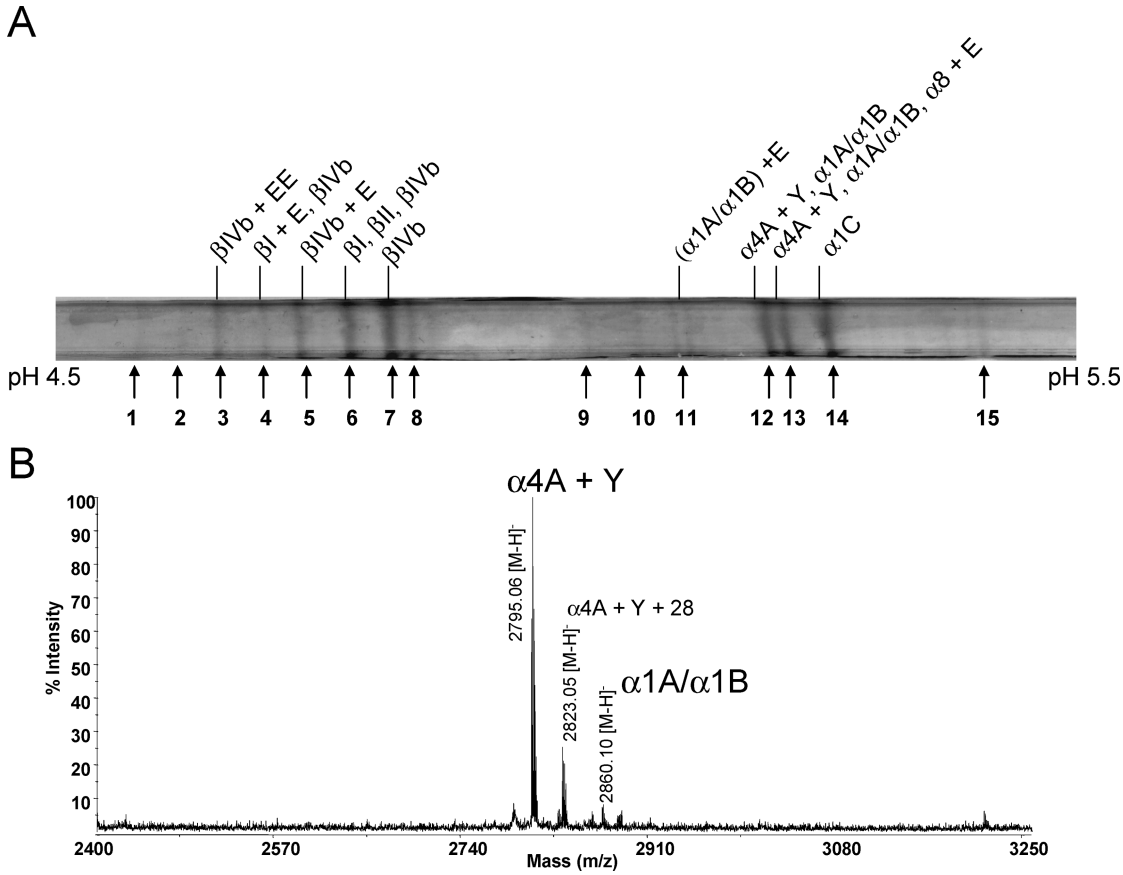

FIGURE 2: Isotype identification by IEF and CNBr cleavage. (A) Region of a 24 cm pH 4.5−5.5 IPG strip showing all the bands that represent different tubulin isotypes in the total tubulin pellet of a sham operated 9 day control liver. Numbered arrows indicate the 15 bands that were cut from the gel. The CNBr-cleaved C-terminal peptides for α1A and α1B isotypes have the same mass; therefore, these two isotypes cannot be distinguished from one another. When a mass is observed that could be either α1A or α1B, it is denoted as α1A/α1B. (B) Mass spectrum obtained after CNBr cleavage of band 12 in panel A. Two α-tubulin isotypes were observed in this band, indicating that there is some overlap of isotypes when using this method. The α4A isotype was tyrosinated (+Y), indicating the post-translational addition of a Tyr residue (+163 Da). The α4A + Y + 28 peak is an artifact, with 28 Da due to formylation from the CNBr cleavage performed in 70% FA.

not include the most intense peak in the spectrum. Instead, a peak at *m/z* 3308.31 was the most intense peak (Figure 3B). Since *β*IVb was identified in the adjacent band, the *β*IVb peak was most likely due to overlap of the bands. Therefore, another form of *β*-tubulin was responsible for the most intense peak. To determine the sequence of this unidentified peptide, it was selected for MS/MS (done in positive ion mode). MS/MS yielded 26 product ions (Figure 3C). These ions, in conjunction with the intact mass of the peptide (3310.31, $[M + H]^+$), were searched in the Mascot database (*30*). Initial searches of the NCBInr (version 20080206) and MSDB (version 20060831) databases did not yield any matches. Next the mouse and other EST databases (version 20080108) were searched, and a sequence was found that matched the MS/MS data, with the correct assignment of 17 b-type and nine y-type ions (Figure 3D) (*31*). This sequence was identical to *β*IVb, except that it was missing the final two amino acids on the C-terminus, valine and alanine. This novel *β*-tubulin C-terminal peptide is denoted as *β** in the remainder of this paper.

Isoelectric Focusing To Identify Tubulin Isotypes in Liver. Four stages of hepatocellular carcinoma were examined by isoelectric focusing. The first stage, 9 days after partial hepatectomy, results in small, preneoplastic nodules, which are estimated to occupy 70% of the area in the liver tissue sections examined, similar to what was previously noted in our laboratory (*27*). In this stage, the noduled tissue was compared to that of a control animal which had undergone a partial hepatectomy (regenerating liver). Analysis by high-resolution IEF and CNBr cleavage revealed that the same tubulin isotypes were present in the 9 day preneoplastic nodule liver and the regenerating liver control animal. Four α-tubulin and four *β*-tubulin isotypes were observed, and some of these forms harbored post-translational modifications such as glutamylation and tyrosination (Table 2 and Figure 4A). In the liver, 4 months after the partial hepatectomy, early persistent nodules account for approximately 35% of the area of the tissue sections that were examined. At this stage, four α-tubulin and three *β*-tubulin isotypes were observed in the early persistent nodule liver as compared to three α-tubulin and three *β*-tubulin isotypes in the sham operated animal of the same age (Table 2). Post-translationally modified forms of both α- and *β*-tubulin were seen in this stage. Six months after the partial hepatectomy, it is estimated that 50% of the cells in a liver section arise from late persistent nodules. At this stage, the animals with late persistent nodules were compared to sham animals of the same age, and four α-tubulin and three *β*-tubulin isotypes were identified in the late persistent nodule livers, some with post-translational modifications (Table 2), whereas three α-tubulin and three *β*-tubulin isotypes were identified in the controls. In the final stage, 10 months after partial hepate-

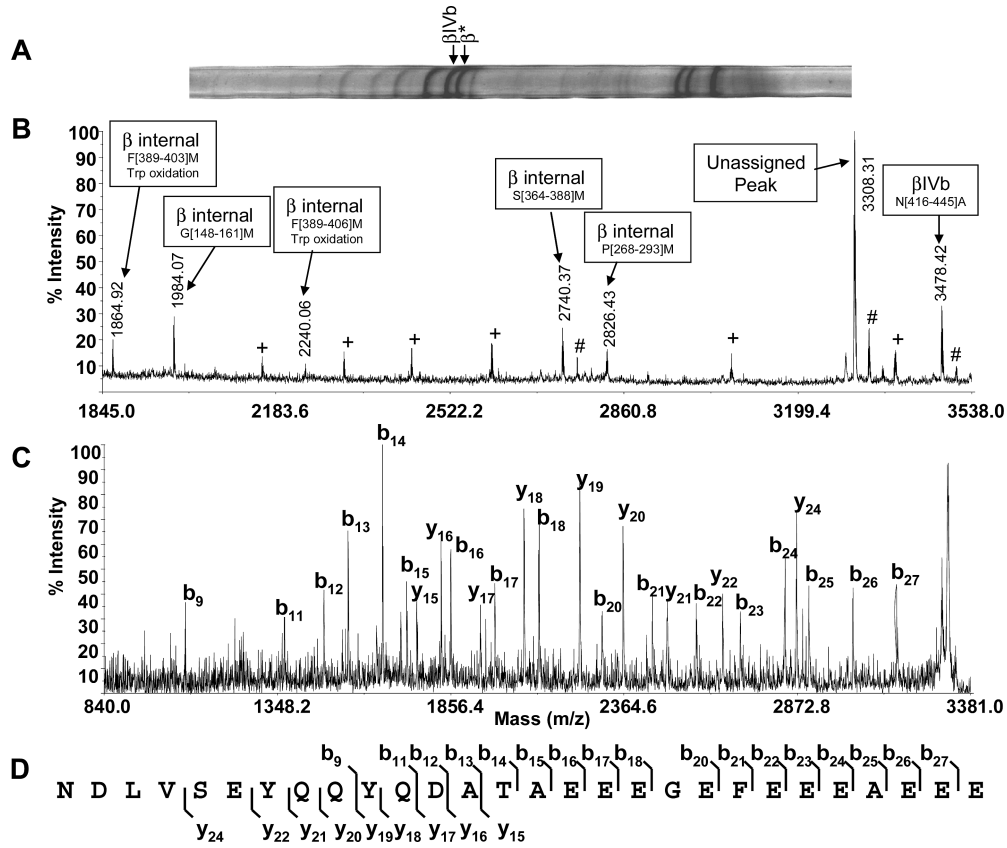

FIGURE 3: Identification of a novel β-tubulin C-terminal peptide. (A) IEF gel of tubulins from tissue with late persistent nodules (6 months after partial hepatectomy). (B) Negative ion mode MS spectrum for CNBr cleavage of the band marked with the arrow in panel A. The higher-intensity peaks were assigned to β-tubulin as shown, except for the highest-intensity peak at 3308.31 Da. This peak was selected for MS/MS. The peaks were assigned on the basis of accurate mass measurements. A plus sign identifies peaks that were not assigned to tubulin peptides, and a number sign identifies formylation (28 Da). (C) MS/MS spectrum for the peak at 3308.31 Da. (D) The MS/MS results were searched in the Mascot database, using an expressed sequence tag (EST) database, and the sequence shown was returned as the best match, with 17 b-type and nine y-type ions identified as indicated.

Table 2: Tubulin Isotypes Identified by High-Resolution Isoelectric Focusing Experiments at Each Stage of Liver Carcinogenesis in the Rat

	βI + EE[c]	βIVb + EE	βI + E	βIVb + E	βI	βII	βIVb	βV	β*	(α1A/α1B) + EE	(α1A/α1B) + E	α4A + Y	α1A/α1B	α8 + E	α1C	(α1A/α1B) − Y
9D RL[a]	+[b]	+	−	+	+	+	+	+	+	−	+	+	+	+	+	−
9D nodules	−	−	+	+	+	+	+	+	+	−	+	+	+	+	+	−
4M sham	−	+	−	+	+	+	+	−	+	−	–	+	+	−	+	+
4M nodules	−	+	−	+	+	+	+	−	+	−	+	+	+	+	+	+
6M sham	+	+	−	+	+	+	+	−	+	−	+	+	+	−	+	−
6M nodules	−	+	+	+	+	+	+	−	+	−	–	+	+	+	+	−
10M sham	−	+	−	+	+	+	+	−	+	−	+	+	+	+	+	−
10M tumor	−	+	+	+	+	+	+	−	+	+	+	+	+	−	+	−
lung sham	−	−	−	+	+	+	+	−	+	+	+	+	+	+	+	+
lung tumor	−	−	+	+	+	+	+	−	+	−	+	+	+	+	+	+

[a] Nine days (9D), 4 months (4M), 6 months (6M), and 10 months (10M) following partial hepatectomy. Nodules refers to animals that underwent the cancer-inducing regimen, and the control animals are regenerating liver (RL 9D) or sham operated (4M, 6M, and 10M). [b] A plus sign indicates that the isotype was observed in that sample, and a minus sign indicates that the isotype was not observed. [c] Post-translational modifications: +E (glutamylation, +129 Da) and ±Y (tyrosination/detyrosination, ±163 Da).

ctomy, tumor cells comprise 70% of the area in the liver sections. At this stage, three α-tubulin and three β-tubulin isotypes were observed in the tumor samples and four α-tubulin and three β-tubulin isotypes were seen in the control animals (Table 2 and Figure 4B). Post-translationally modified forms of βI, βIVb, α1A/α1B, α4A, and α8 were noted.

The unique β-tubulin C-terminal peptide, β*, was present in all stages in both control and nodule or tumor tissue, but the band for the β* form of tubulin was more intense in tissue containing nodules or tumors than in sham livers (Figure 4A,B). This indicated that the level of this post-translationally modified form of βIVb-tubulin was increased in the livers after the animals underwent the cancer-inducing regimen.

Relative Quantitation of the Distinct β-Tubulin C-Terminal Peptide in Liver Cancer. To determine the level of the β* form of tubulin in the nodule or tumor tissue as compared to the control sample, we developed a method employing two ^{15}N-labeled standards (Figure 1). The first peptide had the same sequence as the β* C-terminal CNBr peptide and was synthesized with five ^{15}N-labeled residues, shifting it 5 Da from the naturally occurring β* C-terminal peptide, and the second peptide was an internal peptide common to βI,

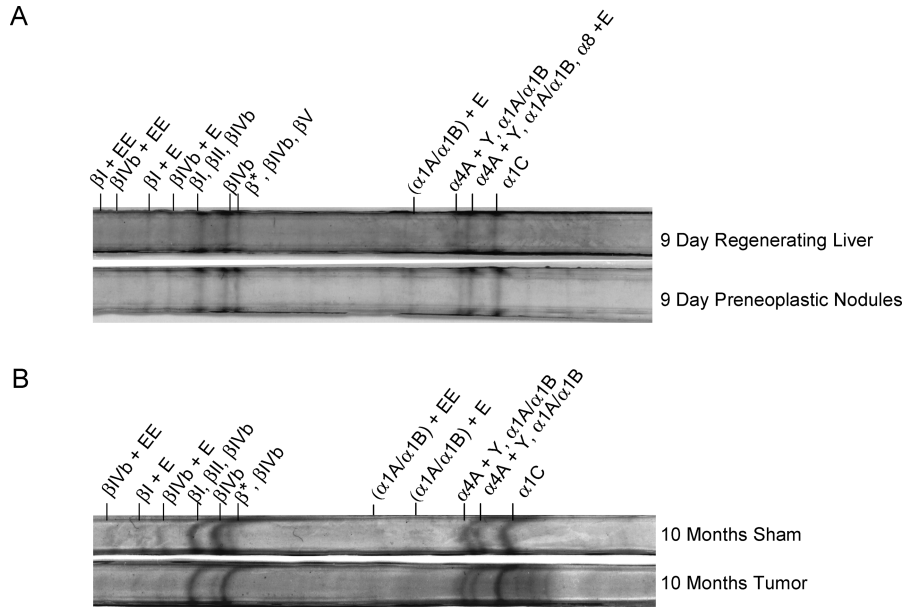

FIGURE 4: High-resolution isoelectric focusing of tubulin from early and late stages of carcinogenesis. (A) Tubulin isotypes identified in control 9 day regenerating liver and 9 day preneoplastic nodule liver. (B) Tubulin isotypes found in 10 month sham control and tumor liver tissue.

βII, βIVb, and βV (residues 148−164) containing three ^{15}N-labeled amino acids. The pellet containing all tubulin isotypes was run on an SDS−PAGE gel, and the band containing total tubulin was cut from the gel after staining. Before cleavage with CNBr, ^{15}N-labeled standards (15 pmol of internal peptide and 6 pmol of C-terminal peptide) were added to the gel bands. Following CNBr fragmentation, these samples were run in negative and positive ion mode on MALDI-TOF/TOF MS. The ratio of sample to standard was determined for both the C-terminal peptide and the internal peptide, with the ratios calculated on the basis of the intensity of the top three (internal, positive ion mode) and five isotopes (C-terminal, negative ion mode) (Figure 5). The internal peptide was then used to standardize the amount of β-tubulin among samples, since this internal peptide was found in all the β-tubulin isotypes that were observed. After correcting for the total amount of β-tubulin using the internal standard, we compared the C-terminal peptide ratio between nodule or tumor samples and control samples (Figure 6).

The β* form of tubulin was present approximately 3-fold more in the preneoplastic liver (9 days after partial hepatectomy) than in the control liver (Figure 6). For livers containing the early persistent nodules, β* was 1.7 times more abundant than in the control sample. In livers with late persistent nodules, the level of modification was again seen to be 3 times that of the control sample, which was also observed in livers with tumors.

Tubulin Isotypes in Lung with Liver Tumor Metastases. In the late stage of liver cancer in humans, liver metastases can be observed in the lung. The resistant hepatocyte rat model of liver cancer produces lung metastases 10 months following partial hepatectomy. The lungs from rats at this stage were examined to determine which tubulin isotypes were present, and these samples were compared to lungs from control animals of the same age. Two animals with tumors and two control animals were examined. The tumor growth in the lung was clearly metastasized from the liver. In the lung with tumors and in the lung of the control animal, we observed four α-tubulin and three β-tubulin isotypes, with modified forms of both α- and β-tubulin present (Table 2). Low levels of the β* form of tubulin were seen in the lungs of sham operated animals, while the amount of the β* form of tubulin was increased in the lungs of animals with liver metastases (data not shown).

DISCUSSION

Tubulin isotypes are highly conserved across species and exhibit tissue-specific expression, although the importance of this expression is not clear (*7*). However, it has been demonstrated that the tubulin isotypes display different assembly dynamics in vitro and that a shift in isotype expression may provide a way for cells to regulate the functions of their microtubules (*8*). Of the α-tubulin isotypes, α1A and α1B are the major isotypes found in the brain but are present at lower levels in many tissues. α1C is a minor isotype that is found in many tissue types, whereas α3A and α3B are testes-specific. The β-tubulin isotypes also have a diverse distribution with βII and βIVa as the major neuronal isotypes, with βII also being expressed in various tissues, whereas βIVa is brain-specific. βIII is a minor neuronal isotype but is neuron-specific. βI, βIVb, and βV are found in many tissues, with βIVb being the major isotype in the testes. βVI is specific for hematopoietic cells (*3, 6*). It has been shown that the amount of specific tubulin isotypes can change in cancer cells, but the studies done to date have focused mainly on β-tubulin isotypes with a recent investigation examining the post-translational modifications of α-tubulin (*12–17*). In this paper, we examined all tubulin isotypes present in early, middle, and late stages of liver cancer and compared them with isotypes from the liver from control animals. We obtained information about both α- and β-tubulin isotypes as well as post-translational modifications, and our experiments indicate that alterations in tubulin isotypes occur during carcinogenesis.

To examine the tubulin isotypes present in liver cancer, we employed a rat model which progresses through well-

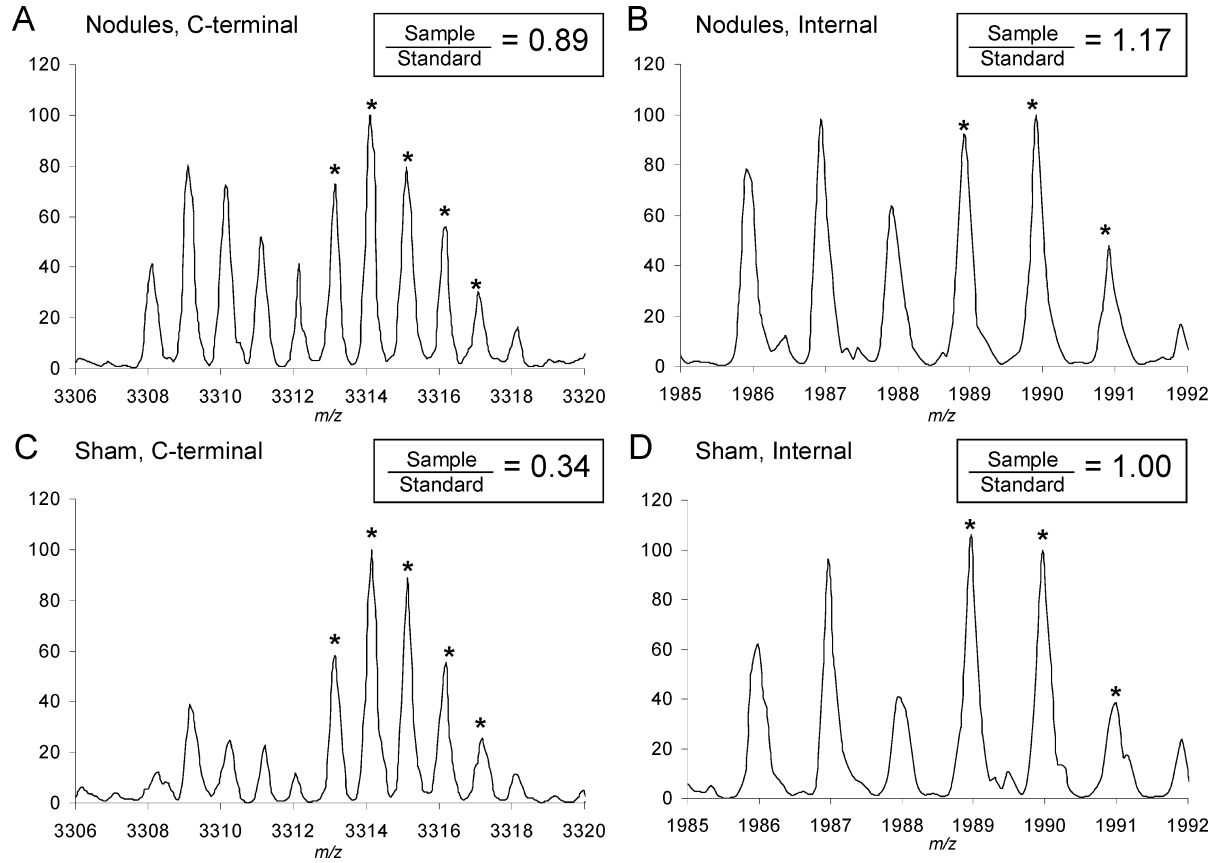

FIGURE 5: Ratio of the β* form of tubulin to total β-tubulin. In panels A and C, the ratio of the C-terminal β* peptide (sample) to the internal C-terminal peptide standard (standard) was determined by adding the peak heights for the top five isotopes for the sample and then dividing by the sum of the peak heights (after correcting for isotope overlap; see Materials and Methods) for the top five isotopes for the standard peptide (indicated with an asterisk). The ratios for each sample to the standard peptide are indicated in the box (sample/standard): (A) 6 month late persistent nodules and (C) 6 month sham. In panels B and D, the ratio of the internal peptide (sample) to the internal peptide standard (standard) was determined by adding the peak heights for the top three isotopes for the sample and then dividing by sum of the top three isotopes for the internal standard peptide (indicated with an asterisk). The ratios for each sample to the standard peptide are indicated in the box (sample/standard): (B) 6 month late persistent nodules and (D) 6 month sham. To obtain the final ratio of β* to total β-tubulin, the ratio obtained for the C-terminal peptide was divided by the ratio for the internal peptide. These numbers are summarized in Figure 6.

defined synchronous stages of liver cancer, similar to the progression of liver cancer in humans. The structural reorganization that occurs in persistent nodule cells and hepatoma cells in the liver of the rat model during carcinogenesis most likely reflects changes in the cytoskeleton. Whereas normal hepatocytes have a characteristic apical-basal polarity and are arranged linearly in hepatic cords, nodule cells lose this polarity and are organized into acinar or glandular-like structures (*27, 32*). Previous studies employing this model have demonstrated changes in levels of expression of cytoskeletal proteins, such as vimentin and actin (*27*). In this study, we focused on tubulins, the proteins that form the microtubule cytoskeleton. The α-tubulin isotypes that were observed in all samples were α1A/α1B, α4A + Y, and α1C, and the β-tubulin isotypes observed in all samples were βI, βII, and βIVb. βV was observed only in early stages, and although it has been suggested that βV and βIII exhibit a complementary pattern of expression, βIII was not seen in these experiments (*23*).

In the high-resolution isoelectric focusing experiments, a band was observed in the region of the β-tubulins that produced a C-terminal peptide upon CNBr cleavage that did not correlate with any of the predicted tubulin isotypes or known modified forms of tubulin. The peptide was subjected to MS/MS, and the data were searched against EST databases, after no results were obtained in protein databases. An EST was identified, which had the same sequence as βIVb minus the last two residues. When the EST was searched against the genomic sequence for rat, it exhibited 100% identity with the gene for βIVb, indicating that the retrieved EST was a fragment of the βIVb gene. The βIVb gene is not known to have any splice variants or SNPs in the C-terminal region that would lead to a shortened sequence. Therefore, the observed peptide is a novel post-translationally truncated form of βIVb-tubulin.

Comparing the intensity of the band for the truncated form of βIVb-tubulin between control and cancerous tissue, we observed that the band stained darker in the samples from livers with nodules or tumors (Figure 4B). Using mass spectrometry to identify and quantitate the relative levels of highly acidic peptides is challenging, especially when using animal or human tissue samples that cannot be directly labeled with heavy isotopes (*33*). To achieve relative quantitation of the novel form of β-tubulin in nodule or tumor tissue relative to control animals, we developed a method that employed two ^{15}N-labeled internal standards. This allowed for relative quantitation of the C-terminal acidic peptide from tubulin and prevented losses that are commonly associated with acidic peptides during reverse phase chromatography (*34*). This method could be applied to other

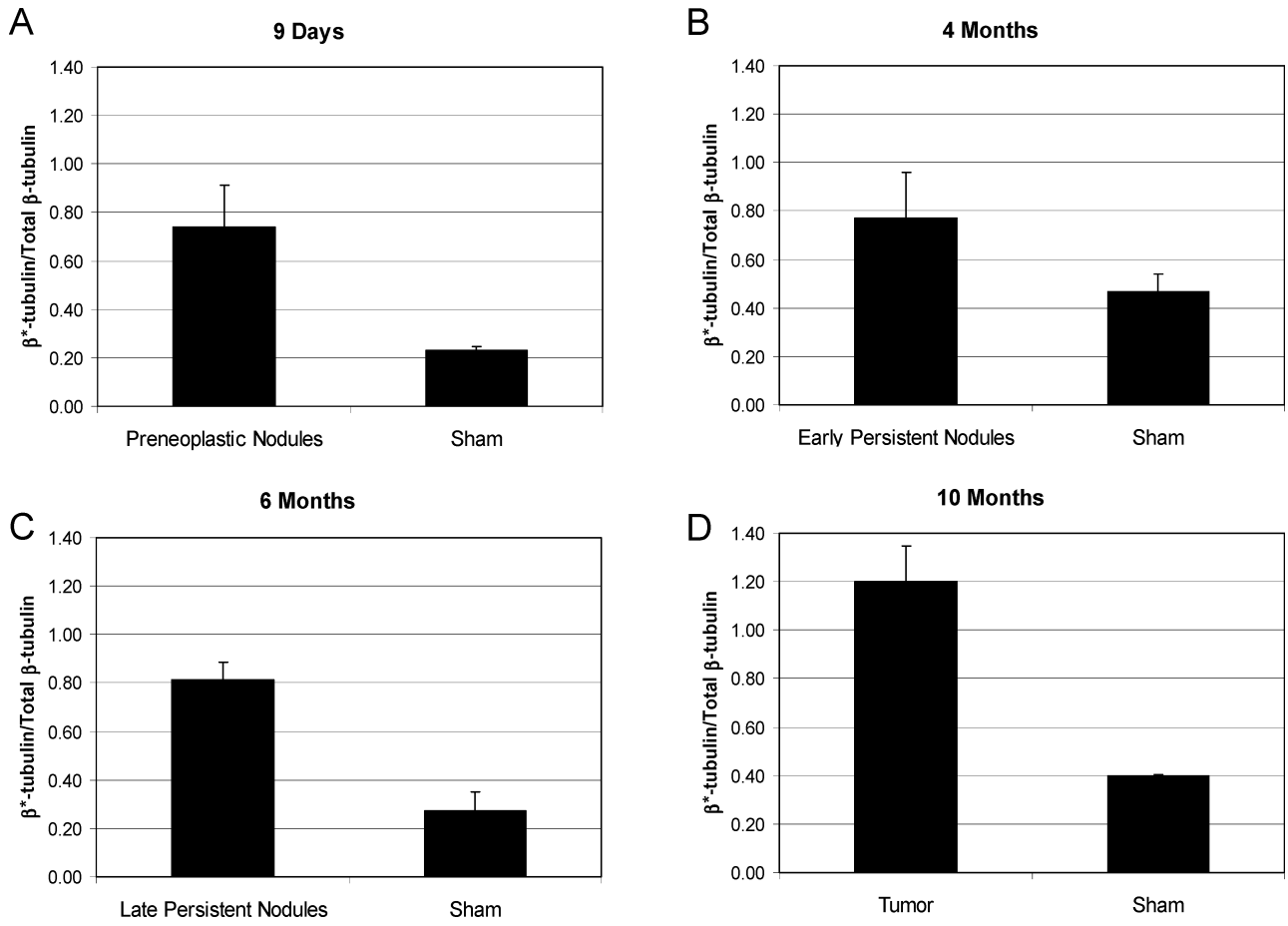

FIGURE 6: Summary of quantitation results. The ratio of the β* form of tubulin in nodule or tumor livers as compared to control livers at each stage. Six different animals were used for each stage (three nodule or tumor and three control), and the values were averaged in each case: (A) 9 days, (B) 4 months, (C) 6 months, and (D) 10 months after partial hepatectomy.

acidic peptides with the synthesis of specific labeled standards. With this method, we determined that in the early stages, the ratio was approximately 3-fold greater in the preneoplastic tissue relative to regenerating liver. In the early persistent nodules, a ratio of 1.7 was observed. This lower ratio could be a result of the decreased amount of altered cells at this stage (~35% of the area of the liver section analyzed was occupied by early persistent nodules, whereas the area covered by the altered cells was greater in the preneoplastic nodule stage and the later stages). However, it is clear that in the later stages, particularly when tumors are found throughout the tissue, there is an approximately 3-fold increase in the amount of the β* form of tubulin present versus that in the control animals (Figure 6).

The C-terminal domain of tubulin accounts for the majority of diversity in microtubules. With this domain located on the outside surface of the microtubules, it has the potential to interact with many proteins that travel along or bind to microtubules. Post-translational modification of the C-terminal tail of tubulin has been demonstrated to modulate the binding of proteins to the microtubules (*35*). Studies have confirmed that the extent of glutamylation can affect the binding of microtubule-associated proteins (*36, 37*). In our experiments, glutamylation was the most commonly observed post-translational modification, occurring on both α- and β-tubulins. The α8-tubulin isotype was observed in many samples but was only observed as the monoglutamylated form and never as the unmodified form. Also, the monoglutamylated form of the βI-tubulin isotype was observed at low levels in liver with nodules or tumors (except in liver with early persistent nodules), but not in the corresponding control animals. The α4A and α8 isotypes are the only α-tubulins without genetically encoded C-terminal tyrosines, but the α4A-tubulin isotype observed in the rat liver was tyrosinated, which occurs enzymatically by a tubulin-tyrosine ligase (TTL) (*38*).

α-Tubulin can undergo a reversible tyrosination/detyrosination event, wherein a TTL adds tyrosine to the C-terminal glutamic acid of α-tubulin and a tubulin carboxypeptidase removes the tyrosine (*38–40*). Furthermore, the penultimate glutamic acid can be removed, resulting in Δ2-tubulin, which is eliminated from the tyrosination cycle (*41*). Although the protease responsible for the removal of the penultimate glutamic acid has not yet been identified, it is known to be a specific process and not due to random proteolysis (*5, 42*). Tyrosinated tubulin is commonly found in cycling cells, whereas detyrosinated tubulin and Δ2-tubulin are found in stable microtubules (*42, 43*). Recently, it was demonstrated that detyrosinated tubulin and Δ2-tubulin occur more frequently in tumors than in normal tissue which is thought to be due to suppression of TTL (*44, 45*). Previously, no modification in which residues are removed from the C-terminus of β-tubulin had been described. In this paper, we provide the first evidence of a novel form of βIVb-tubulin in which the last two residues of the C-terminal tail have been removed. This modification exposes a charged C-terminal glutamic acid residue instead of the genetically encoded hydrophobic residues, valine and alanine. In the later

stages of liver cancer, the majority of the βIVb isotype is converted to this truncated form (Figure 4B). Since the βIVb isotype is one of the major β-tubulin isotypes present in the liver, this modification of its C-terminal region could change the proteins that interact with microtubules. It is likely that enhanced levels of the novel form of βIVb-tubulin in liver cancer is due to increased protease activity in the premalignant and malignant stages, although database searches do not reveal any known proteases for this specific cleavage site (http://merops.sanger.ac.uk/) (*46*). Recently, a novel class of cytosolic carboxypeptidases has been identified which may include the protease undertaking the removal of the C-terminal tyrosine in α-tubulin (*47, 48*). Furthermore, these proteases can cleave a variety of C-terminal amino acids from synthetic peptides, indicating that they may have a broader function than the removal of C-terminal tyrosines and could potentially be responsible for the removal of hydrophobic residues from the C-terminus of βIVb-tubulin. Proteases have been shown to play an important role in tumor metastasis and in tumor development and can be used as biomarkers and as targets for anticancer agents (*49*). The upregulation/activation of the enzyme responsible for this unique post-translational modification of βIVb-tubulin could potentially serve as a biomarker for early stages of HCC development.

The role of tubulin isotypes in cancer is not well understood, but studies continue to identify the changes that take place in tubulin isotype expression and modification in cancer. It is known that isotype expression can affect the assembly of microtubules as well as modulate their sensitivity to drugs. Furthermore, alterations in tubulin can affect the endogenous proteins that interact with microtubules. Therefore, it is important to understand the changes that occur within the cytoskeleton during carcinogenesis. In this paper, we provide a comprehensive profile of the tubulin isotypes present in normal liver and liver cancer in the rat. A novel post-translational modification of the βIVb-tubulin isotype is also described. This unique βIVb-tubulin form is present at higher levels in the livers of animals that have undergone the experimental regimen. Our observations also emphasize the need to identify specific tubulin-modifying enzymes, such as proteases, as potential markers of tumors or as therapeutic targets. Future studies in our laboratory are aimed at profiling tubulin isotypes present in human cancers of diverse origins and identifying post-translational modifications of the β-tubulins.

ACKNOWLEDGMENT

We thank Ms. Berta Burd for her assistance in the purification of tubulin and for her helpful advice. We also thank Dr. Tom W. Muir for his assistance with the synthesis of the peptide standards.

REFERENCES

1. Desai, A., and Mitchison, T. J. (1997) Microtubule polymerization dynamics. *Annu. Rev. Cell Dev. Biol. 13*, 83–117.
2. Nogales, E. (2000) Structural insights into microtubule function. *Annu. Rev. Biochem. 69*, 277–302.
3. Luduena, R. F. (1998) Multiple forms of tubulin: Different gene products and covalent modifications. *Int. Rev. Cytol. 178*, 207–275.
4. Sullivan, K. F., and Cleveland, D. W. (1986) Identification of conserved isotype-defining variable region sequences for four vertebrate β-tubulin polypeptide classes. *Proc. Natl. Acad. Sci. U.S.A. 83*, 4327–4331.
5. Westermann, S., and Weber, K. (2003) Post-translational modifications regulate microtubule function. *Nat. Rev. Mol. Cell Biol. 4*, 938–947.
6. Sullivan, K. F. (1988) Structure and utilization of tubulin isotypes. *Annu. Rev. Cell Biol. 4*, 687–716.
7. Luduena, R. F. (1993) Are tubulin isotypes functionally significant. *Mol. Biol. Cell 4*, 445–457.
8. Panda, D., Miller, H. P., Banerjee, A., Luduena, R. F., and Wilson, L. (1994) Microtubule dynamics in vitro are regulated by the tubulin isotype composition. *Proc. Natl. Acad. Sci. U.S.A. 91*, 11358–11362.
9. Orr, G. A., Verdier-Pinard, P., McDaid, H., and Horwitz, S. B. (2003) Mechanisms of Taxol resistance related to microtubules. *Oncogene 22*, 7280–7295.
10. Verhey, K. J., and Gaertig, J. (2007) The tubulin code. *Cell Cycle 6*, 2152–2160.
11. Gan, P. P., Pasquier, E., and Kavallaris, M. (2007) Class III β-tubulin mediates sensitivity to chemotherapeutic drugs in non small cell lung cancer. *Cancer Res. 67*, 9356–9363.
12. Kavallaris, M., Kuo, D. Y., Burkhart, C. A., Regl, D. L., Norris, M. D., Haber, M., and Horwitz, S. B. (1997) Taxol-resistant epithelial ovarian tumors are associated with altered expression of specific beta-tubulin isotypes. *J. Clin. Invest. 100*, 1282–1293.
13. Katsetos, C. D., Herman, M. M., and Mork, S. J. (2003) Class III β-tubulin in human development and cancer. *Cell Motil. Cytoskeleton 55*, 77–96.
14. Lee, K. M., Cao, D., Itami, A., Pour, P. M., Hruban, R. H., Maitra, A., and Ouellette, M. M. (2007) Class III β-tubulin, a marker of resistance to paclitaxel, is overexpressed in pancreatic ductal adenocarcinoma and intraepithelial neoplasia. *Histopathology 51*, 539–546.
15. Seve, P., Isaac, S., Tredan, O., Souquet, P. J., Pacheco, Y., Perol, M., Lafanechere, L., Penet, A., Peiller, E. L., and Dumontet, C. (2005) Expression of class III β-tubulin is predictive of patient outcome in patients with non-small cell lung cancer receiving vinorelbine-based chemotherapy. *Clin. Cancer Res. 11*, 5481–5486.
16. Oda, E., Nakamura, Y., Yamamoto, M., and Kojiro, M. (2005) Immunohistochemical distribution of tubulin βII in human normal and neoplastic tissues. *Kurume Med. J. 52*, 117–125.
17. Soucek, K., Kamaid, A., Phung, A. D., Kubala, L., Bulinski, J. C., Harper, R. W., and Eiserich, J. P. (2006) Normal and prostate cancer cells display distinct molecular profiles of α-tubulin posttranslational modifications. *Prostate 66*, 954–965.
18. Verdier-Pinard, P., Wang, F., Burd, B., Angeletti, R. H., Horwitz, S. B., and Orr, G. A. (2003) Direct analysis of tubulin expression in cancer cell lines by electrospray ionization mass spectrometry. *Biochemistry 42*, 12019–12027.
19. Alexander, J. E., Hunt, D. F., Lee, M. K., Shabanowitz, J., Michel, H., Berlin, S. C., MacDonald, T. L., Sundberg, R. J., Rebhun, L. I., and Frankfurter, A. (1991) Characterization of posttranslational modifications in neuron-specific class III β-tubulin by mass spectrometry. *Proc. Natl. Acad. Sci. U.S.A. 88*, 4685–4689.
20. Vinh, J., Langridge, J. I., Bre, M. H., Levilliers, N., Redeker, V., Loyaux, D., and Rossier, J. (1999) Structural characterization by tandem mass spectrometry of the posttranslational polyglycylation of tubulin. *Biochemistry 38*, 3133–3139.
21. Verdier-Pinard, P., Wang, F., Martello, L., Burd, B., Orr, G. A., and Horwitz, S. B. (2003) Analysis of tubulin isotypes and mutations from taxol-resistant cells by combined isoelectrofocusing and mass spectrometry. *Biochemistry 42*, 5349–5357.
22. Rao, S., Aberg, F., Nieves, E., Horwitz, S. B., and Orr, G. A. (2001) Identification by mass spectrometry of a new α-tubulin isotype expressed in human breast and lung carcinoma cell lines. *Biochemistry 40*, 2096–2103.
23. Verdier-Pinard, P., Shahabi, S., Wang, F., Burd, B., Xiao, H., Goldberg, G. L., Orr, G. A., and Horwitz, S. B. (2005) Detection of human βV-tubulin expression in epithelial cancer cell lines by tubulin proteomics. *Biochemistry 44*, 15858–15870.
24. Solt, D. B., Medline, A., and Farber, E. (1977) Rapid emergence of carcinogen-induced hyperplastic lesions in a new model for the sequential analysis of liver carcinogenesis. *Am. J. Pathol. 88*, 595–618.
25. Garcia, M., Jemal, A., Ward, E. M., Center, M. M., Hao, Y., Siegel, R. I., and Thun, M. J. (2007) Global Cancer Facts & Figures 2007, American Cancer Society, New York.

26. Farazi, P. A., and DePinho, R. A. (2006) Hepatocellular carcinoma pathogenesis: From genes to environment. *Nat. Rev. Cancer 6*, 674–687.
27. Luo, Q., Siconolfi-Baez, L., Annamaneni, P., Bielawski, M. T., Novikoff, P. M., and Angeletti, R. H. (2007) Altered protein expression at early-stage rat hepatic neoplasia. *Am. J. Physiol. 292*, G1272−G1282.
28. Lapatsanis, L., Milias, G., Froussios, L., and Kolovos, M. (1983) Synthesis of N-(2,2,2-trichloroethoxycarbonyl) L-amino acids and N-(9-fluorenylmethoxycarbonyl) L-amino acids involving succinimidoxy anion as a leaving group in amino acid protection. *Synthesis 8*, 673–673.
29. Kempe, T., Chow, F., Peterson, S. M., Baker, P., Hays, W., Opperman, G., L'Italien, J. J., Long, G., and Paulson, B. (1986) Production and Characterization of Growth Hormone Releasing Factor Analogs Through Recombinant DNA and Chemical Techniques. *Nat. Biotechnol. 4*, 565–568.
30. Perkins, D. N., Pappin, D. J., Creasy, D. M., and Cottrell, J. S. (1999) Probability-based protein identification by searching sequence databases using mass spectrometry data. *Electrophoresis 20*, 3551–3567.
31. Boguski, M. S., Lowe, T. M., and Tolstoshev, C. M. (1993) dbEST: Database for "expressed sequence tags". *Nat. Genet. 4*, 332–333.
32. Farber, E., Cameron, R. G., Laishes, B., Lin, J.-C., Medline, A., Ogawa, K. , and Solt, D. B. (1979) in *Carcinogens: Identification and Mechanisms of Action* (Griffin, A. C., and S., R. S., Eds.) pp 319−335, Raven Press, New York.
33. van Dijk, J., Miro, J., Strub, J. M., Lacroix, B., van Dorsselaer, A., Edde, B., and Janke, C. (2008) Polyglutamylation is a post-translational modification with a broad range of substrates. *J. Biol. Chem. 283*, 3915–3922.
34. Regnard, C., Desbruyeres, E., Huet, J. C., Beauvallet, C., Pernollet, J. C., and Edde, B. (2000) Polyglutamylation of nucleosome assembly proteins. *J. Biol. Chem. 275*, 15969–15976.
35. Rosenbaum, J. (2000) Cytoskeleton: Functions for tubulin modifications at last. *Curr. Biol. 10*, R801−R803.
36. Bonnet, C., Boucher, D., Lazereg, S., Pedrotti, B., Islam, K., Denoulet, P., and Larcher, J. C. (2001) Differential binding regulation of microtubule-associated proteins MAP1A, MAP1B, and MAP2 by tubulin polyglutamylation. *J. Biol. Chem. 276*, 12839–12848.
37. Larcher, J. C., Boucher, D., Lazereg, S., Gros, F., and Denoulet, P. (1996) Interaction of kinesin motor domains with α- and β-tubulin subunits at a τ-independent binding site. Regulation by polyglutamylation. *J. Biol. Chem. 271*, 22117–22124.
38. Raybin, D., and Flavin, M. (1977) Enzyme which specifically adds tyrosine to the α chain of tubulin. *Biochemistry 16*, 2189–2194.
39. MacRae, T. H. (1997) Tubulin post-translational modifications: Enzymes and their mechanisms of action. *Eur. J. Biochem. 244*, 265–278.
40. Ersfeld, K., Wehland, J., Plessmann, U., Dodemont, H., Gerke, V., and Weber, K. (1993) Characterization of the tubulin-tyrosine ligase. *J. Cell Biol. 120*, 725–732.
41. Paturle-Lafanechere, L., Edde, B., Denoulet, P., Van Dorsselaer, A., Mazarguil, H., Le Caer, J. P., Wehland, J., and Job, D. (1991) Characterization of a major brain tubulin variant which cannot be tyrosinated. *Biochemistry 30*, 10523–10528.
42. Paturle-Lafanechere, L., Manier, M., Trigault, N., Pirollet, F., Mazarguil, H., and Job, D. (1994) Accumulation of δ2-tubulin, a major tubulin variant that cannot be tyrosinated, in neuronal tissues and in stable microtubule assemblies. *J. Cell Sci. 107*, 1529–1543.
43. Gundersen, G., Khawaja, S., and Bulinski, J. (1987) Postpolymerization detyrosination of α-tubulin: A mechanism for subcellular differentiation of microtubules. *J. Cell Biol. 105*, 251–264.
44. Mialhe, A., Lafanechere, L., Treilleux, I., Peloux, N., Dumontet, C., Bremond, A., Panh, M.-H., Payan, R., Wehland, J., Margolis, R.-L., and Job, D. (2001) Tubulin Detyrosination Is a Frequent Occurrence in Breast Cancers of Poor Prognosis. *Cancer Res. 61*, 5024–5027.
45. Lafanechere, L., Courtay-Cahen, C., Kawakami, T., Jacrot, M., Rudiger, M., Wehland, J., Job, D., and Margolis, R. L. (1998) Suppression of tubulin tyrosine ligase during tumor growth. *J. Cell Sci. 111* (2), 171–181.
46. Rawlings, N. D., Morton, F. R., Kok, C. Y., Kong, J., and Barrett, A. J. (2008) MEROPS: The peptidase database. *Nucleic Acids Res. 36*, D320−D325.
47. Kalinina, E., Biswas, R., Berezniuk, I., Hermoso, A., Aviles, F. X., and Fricker, L. D. (2007) A novel subfamily of mouse cytosolic carboxypeptidases. *FASEB J. 21*, 836–850.
48. Rodriguez de la Vega, M., Sevilla, R. G., Hermoso, A., Lorenzo, J., Tanco, S., Diez, A., Fricker, L. D., Bautista, J. M., and Aviles, F. X. (2007) Nna1-like proteins are active metallocarboxypeptidases of a new and diverse M14 subfamily. *FASEB J. 21*, 851–865.
49. Koblinski, J. E., Ahram, M., and Sloane, B. F. (2000) Unraveling the role of proteases in cancer. *Clin. Chim. Acta 291*, 113–135.
50. Khodiyar, V. K., Maltais, L. J., Sneddon, K. M. B., Smith, J. R., Shimoyama, M., Cabral, F., Dumontet, C., Dutcher, S. K., Harvey, R. J., Lafanechere, L., Murray, J. M., Nogales, E., Piquemal, D., Stanchi, F., Povey, S., and Lovering, R. C. (2007) A revised nomenclature for the human and rodent α-tubulin gene family. *Genomics 90*, 285–289.

BI8005225